Effects of non-conventional sterilization methods on PVA-Zylon hydrogels for cartilage repair

Tomás Pires[1], Ana Paula Serro[1,2], Diana Silva Pereira[1,2]

[1] Centro de Química Estrutural, Instituto Superior Técnico, ULisboa, Lisboa, Portugal

[2] Centro de investigação Interdisciplinar Egas Moniz, Instituto Superior de Ciências da Saúde Egas Moniz, Caparica, Portugal

November 2021

Abstract

Articular cartilage (AC) degradation is a recurrent pathology that affects millions of people worldwide. Being an avascular tissue it shows limited healing capacity, and current therapeutic strategies show several limitations. Hydrogels have gained great attention as possible cartilage substitutes, due to their biocompatibility and high water contents. Poly-vinyl alcohol (PVA) is considered one of the most promising hydrogels, however its mechanical properties hinder their application. Reinforcement of the PVA is required to tailor the hydrogels' mechanical properties. To be used in a clinical setting, biomaterials must undergo an effective sterilization. Common sterilization methods such as autoclaving can degrade heat sensitive PVA hydrogels, which justify the need to develop alternative sterilization procedures.

In this work, a novel PVA hydrogel, reinforced with Zylon nanofibers obtained by cast-drying (CD) underwent three non-conventional sterilization methods (i.e., microwave irradiation (MW), high hydrostatic pressure (HHP) and Argon plasma glow discharge). All methods proved capable of sterilizing the material, but led to changes in its properties. MW increased the amount of double bonds, and improved the tested mechanical and tribological properties. HHP increased H-bonding, which improved the tested properties, except but the compressive stiffness at high loads. Plasma treatment resulted in breakage of bonds, thus decreasing the PVA-Zylon's tribological and load bearing capabilities, but improved both the tensile and shear resistance. None of the sterilization methods induced cytotoxicity. PVA-Zylon hydrogels after MW proved to be the most promising materials for cartilage substitution.

Keywords: Cartilage, hydrogel sterilization, PVA, microwave, high hydrostatic pressure, plasma.

1. Introduction

AC is a highly hydrated connective tissue that covers the ends of bones in diarthrodial joints. It consists of a dense extracellular matrix (ECM) composed of a biphasic network of collagen fibers, glycosaminoglycans, proteoglycans, glycoproteins, water and electrolytes. This ECM is populated by a low volume of cells (chondrocytes) and has a limited capacity for healing due to its lack of blood and lymphatic vessels [1]. AC shows an elaborate compartmentalized structure, histologically arranged in distinct zones [2]. This unique structure, in conjugation with a synergistic interaction between the AC tissue and the synovial fluid (SF), provides remarkable biotribological systems, able to withstand large loads while exhibiting extremely low coefficients of friction (CoF) and almost no wear. AC can operate in different lubrication regimes: a) boundary lubrication (BL); b) mixed lubrication (ML) and c) fluid film lubrication (FL). BL regime is characterized by a monolayer of fluid film between the contacting surfaces, and usually occurs in heavy loads and low shear rate conditions [3]. In the ML regime, the opposing surfaces can be either in direct contact or completely separated by a thick fluid film. FL occurs at low applied forces or high sliding speeds, and is characterized by thicker lubricating layers, in which the applied loads are dissipated by elastohydrodynamic forces in the fluid (decreasing CoF) [4]. AC is capable of bearing large applied loads, due to its biphasic and viscoelastic nature. Its elastic component grants it enough stiffness to support static load of the joints while the viscous component provides damping of dynamic forces during movement [5]. With this, AC is able to resist compressive, tensile and shear loads.

In the event of physical injury or disease, the ability of AC to repair and regenerate is limited, due to its aneural and avascular nature [6]. So far, there is no cure for cartilages' degradation, and no satisfactory approach that can duplicate the normal tissue in a reduced post-operative period, capable of sustaining load at an early implementation state, while being cost-effective [7]. Hence, there is an increase need for potential AC substitutes to treat the most severe lesions.

Hydrogels have been studied as cartilage replacement materials, as they are capable of replicating the unique structure of AC, owing to high water contents, porous structure and viscoelastic mechanical properties [8]. PVA hydrogels have emerged as promising candidates, due to their excellent biocompatibility and chemical stability [9]. Nevertheless, their mechanical and lubrication behavior is inferior to that of natural cartilage [10]. One strategy to overcome this is to reinforce PVA hydrogels. Namely, with the addition of nano/micro fibers to the polymer network, mimicking the collagen fibers present in the ECM. Poly(p-phenylene-2,6-benzobisoxazole) (PBO) (trade name Zylon^{TM}), a synthetic rigid-rod polymer fiber with extremely high tensile resistance was used in this work [11].

In order to be used in a clinical setting, implantable

biomaterials sterilization (SZ) is mandatory. Steam heat is one of the most used methods of SZ due to its simplicity and easy access. However, PVA hydrogels are generally sensitive to heat, degrading or suffering significant changes [12]. Gamma ray irradiation is also a commonly used SZ procedure, but the highly energetic radiation use demands specialized equipment and personnel [13]. Thus, there is a need for developing alternative SZ methods. In this work three non-conventional SZ methods were studied (i.e, microwave (MW) irradiation, high hydrostatic pressure (HHP), and reactive plasma exposure).

MW irradiation has been shown to be capable of removing a wide range pathogens in biomaterials in their final packaging [14]. The effects of MW radiation in dipolar substances, particularly water, allow it to achieve high temperatures with a great efficiency and speed [15]. Hence, moist heat SZ is achieved at lower processing times, reducing possible thermal degradation of the materials. Furthermore, it presents low costs (of both equipment and energy requirements), great accessibility, there is no need for toxic chemical components, which precludes toxic or hypersensitivity complications, and is a user-friendly technique.

The HHP method is widely used in the food processing industry, as it does not rely on chemicals, heat or irradiation to destroy pathogens. Instead, water is used to apply high pressures (usually in the range of 100-1000 MPa), that compress the product uniformly and rapidly. The range of temperatures of this process can be adjusted between 0ºC and 100ºC , with exposures time ranging from a few seconds to over 20 min [16]. HHP SZ has proved capable of sterilizing hydrogels (600 MPa, 70ºC during 10 min) [17].

Low-temperature glow discharge plasma treatment has also been investigated for its potential to sterilize polymeric materials. Plasma SZ consists in exposing the materials to free radicals created during the electric discharge in a gas, eroding cellular material [18]. A wide range of discharge gases has been used with positive results, with more reactive gases usually showing higher degrees of SZ, but also creating more toxic residues [19]. Argon (Ar) gas plasma particularly, has the benefit of being inert, and has been shown to be capable of sterilizing biomaterials [18].

In the present work, a PVA-Zylon hydrogel was synthesized by cast-drying (CD). The hydrogel was subjected to non-conventional SZ methods, and the SZ efficacy was evaluated. Extensive characterization of the PVA-Zylon hydrogel properties was carried out to evaluate its applicability as a cartilage replacement material. Additionally, non-sterilized and sterilized materials were compared to evaluate possible effects of the SZ procedures. Finally, biocompatibility of the hydrogels was ascertained via irritability (HET-CAM test) and cytotoxicity assays.

2. Experimental

2.1. Materials

PVA powder (99% hydrolized, MW=146,000-186,000), CASO Broth (Soybean Casein digest Broth), phosphate buffer solution (PBS, pH 7.4, buffer strength=150 mM) and Dulbecco's Modified Eagle's Medium (DMEM) and dimethyl sulfoxide (DMSO) were all obtained from Sigma-Aldrich. Trifluoroacetic acid (TFA) (CF_3COOH) and 99% extra pure methanesulfonic acid (MSA) (CH_4O_3S, MW=96.10), were purchased from CARLO ERBA Reagents and Acros Organics, respectively. Zylon^{TM} (PBO) fibers (type: AS) were obtained from Toyobo Co. Ltd., Japan. Thioglycollate Liquid Medium (TIO) and Sodium chloride (purity $\geq$ 99%, NaCl) were purchased from PanReac (Spain), and sodium hydroxide (purity $\geq$ 99%, NaOH) was obtained from Merck (USA). Special sealed bags (poly-amide and polyethylene, 90 m, 10×10 cm2) were purchased from Penta Iberica and pure argon gas was supplied from a compressed gas bottle at 20 MPa pressure (ALPHAGAZ^{TM} Ar, from Air Liquide). Distilled and deionized (DD) water (18 MΩ cm, pH 7.7) was obtained with a Millipore water purifying system. The weighing of materials was performed in a semi-micro analytical balance OHAUS (Model Discovery DV215CD). Simulated synovial fluid (SSF) was formulated with hyaluronic acid sodium salt (HA), with an average molecular weight of 1–2 million Da (3 mg/mL) and lyophilized bovine serum albumin (BSA), Fraction V, pH 7 (4 mg/mL), dissolved in PBS. The HA and BSA were individually supplied by Carbosynth (Compton, Berkshire, UK) and Serva Electrophoresis GmbH (Heidelberg, Germany). SSF was stored in a refrigerator at 4ºC between each use. Cartilage pins were harvested from porcine cartilage, obtained from a local butcher's shop. Full-depth osteochondral plugs (ϕ = 6 mm) were collected using 6 mm hole punchers on randomly selected sites. The cartilage surface was carefully cut with a scalpel, to prevent sharp edges, washed in DD water and stored at -20 ªC in PBS solution between uses.

2.2. Production of PVA-Zylon Hydrogel

6% w/v PVA powder was mixed with 100% TFA. 1% w/v Zylon fibers were mixed with a 80%TFA, and 20% MSA solution. Both solutions were left with a magnetic stirrer until complete dissolution of the polymers, after which time, the vials are placed in a warm bath (45ºC) for 30 minutes, to decrease the viscosity of the solutions and facilitate mixing. Then, the solutions were mixed vigorously, placed in closed borosylicate petri dishes, and left to rest for 1 hour. Afterwards, airflow was permitted to enter the dish by elevating the lid, and left for a further 2 hours. Following, the lid was completely removed, and the gel was left for 24 hours at room temperature. After complete gelation, the hydrogel was placed in DD water, which was replaced periodically remove acidic solvents, until the pH=7 ($\approx$7days). The washed samples were placed in an oven at 45ºC for at least 48 hours, to finalize the crosslinking process.

2.3. Sterilization

MW SZ was performed using a household 2450 MHz MW oven (Kunft KMW-1698), at 700 W for 3 and 5 minutes. Hydrogel samples were placed in special sealed bags, with $\approx$3 mL of DD water to avoid dehydration, and aid in the sterilizing effect of the MW radiation.

HHP sterilization was carried out in a specialized high pressure equipment (Hiperbaric 55, Burgos, Spain). Preparation of the samples was similar to that of the MW sterilization process. The samples were sterilized

at 70ºC and 600 MPa for 10 minutes.

Plasma sterilization was performed using a compact Harrick PDC-32G Plasma Cleaner/Sterilizer (115 V). The equipment was connected to a gas-compatible oil-based vacuum pump (LVO 100, Leybold), in order to pump nonreactive Ar gas into the chamber. Dry hydrogel samples were placed into the quartz glass chamber, which was then vacuum closed, and connected to the Ar gas bottle. The hydrogels were exposed for 5 minutes at maximum settings (18 W). To avoid contamination, all surfaces in the immediate vicinity of the equipment were disinfected with 70% ethanol and a bunsen burner was strategically placed to ensure an aseptic environment. The chamber was then opened and the samples were carefully placed into previously sterilized falcon tubes containing DD water, using sterilized tweezers.

2.4. Sterility Assessment

SZ was determined through the direct inoculation method. TIO, for potential bacterial growth and CASO-Broth, for fungal growth were prepared in Schott flasks, and sterilized in an autoclave at 121ºC, 10^5 Pa for 20 minutes. Sterilized hydrogels with a diameter of 8 mm were placed into the flasks containing 100 mL of growth medium. Two positive controls for bacterial contamination were created through inoculation of *Pseudomonas aeruginosa* (ATCC 15442) and *Staphylococcus aureus* (ATCC 6538) in the flasks containing TIO medium. A positive control for fungal contamination was created with inoculation of *Candida albicans* (ATCC 10231) in a flask containing CASO medium. As negative controls two flasks, each containing only one of sterilized mediums. All prepared flasks were incubated for 14 days, at 35ºC for TIO medium, and at 25ºC for CASO. Validation of sterility was performed by comparing the samples' incubated flasks with both the positive and negative controls. For each method of sterilization, three replicates of hydrogel material were tested for each medium.

2.5. Microstructure Analysis

The materials' chemical structure was studied through Fourier transform infrared spectroscopy (FTIR) with attenuated total reflectance (ATR). A Spectrum Two from PerkinElmer (Waltham, MA, USA) FTIR equipment equipped with a lithium tantalite (LiTaO3) mid-infrared (MIR) detector (signal/noise ratio 9300:1) and a UATR Two accessory was used. A diamond ATR crystal was utilized to control the applied force ensuring good contact between the crystal and samples. All obtained spectra were normalized ("Normalize" function, normalize method [0,1]) using the OriginPro 8.5 software, collected at 4 cm^{-1} resolution and 8 scans of data accumulation were carried out.

Dry 14 mm disk of each hydrogel condition were used for this analysis. Plasma treated samples were cut, separating the surface from the bulk, to determine differences across the hydrogel's depth.

2.6. Swelling

Hydrogel disks with 6 mm diameter were dried for 2 days at 45ºC before being weighted (dry weight, W_d). Afterwards, the hydrogels were placed in 5 mL of DD water, incubated at 37ºC and periodically weighted (wet weight, W_h) until a constant value was achieved. The samples were carefully blotted with absorbent paper before each measurement to remove any remaining water droplets from their surface. The swelling capacity (SC) was calculated along the tested time range (120 hours) and the water content (WC) was calculated at equilibrium, using the following equations:

$$SC(\%) = \frac{W_h - W_d}{W_d} * 100 \quad (1)$$

$$WC(\%) = \frac{W_h - W_d}{W_h} * 100 \quad (2)$$

2.7. Compressive and Tensile Testing

Compressive tests were performed using a TA.XT Express Texture Analyzer (Stable Micro Systems). Uniaxial compression was performed with a load cell of 49 N in unconfined mode. Hydrated 8mm diameter samples, with a thickness of ≈4mm were immersed in DD water at room temperature, and compressed at a strain rate of 0.1 mm·s^{-1}, up to a 40% strain of the material. Each hydrogel sample underwent several cycles of loading-unloading, until the hysteresis curves were deemed reproducible (5 cycles)..

Tensile resistance tests were performed in the same equipment with a force of 49 N at a speed of 0.5 mm/s in hydrated dumbbell-shaped specimens of hydrogel (5 mm width, 2.5 mm gauge width, 8 mm gauge length, total length 18 mm).

Compressive (E_c) and tensile (E_t) Young's Modulus were measured at the initial linear portion of the stress-strain (σ/ϵ) curves, at 1% strain, using the standard Young's modulus equation:

$$E = \frac{\sigma}{\epsilon} \quad (3)$$

The tangent compressive and tensile modulus (E_ϵ) were calculated in the strain range of 5-35%, in 5% increments by the finite difference method [20], according to the obtained stress-strain curves, expressed with the following equation:

$$E_\epsilon = \frac{\sigma_{\epsilon+\Delta\epsilon} - \sigma_{\epsilon-\Delta\epsilon}}{2\Delta\epsilon} \quad (4)$$

where E_ϵ is the tangent modulus of the hydrogel at the strain ratio value of ϵ. The difference in strain value $\Delta\epsilon$ was 1%.

2.8. Rheology

Rheological measurements were performed in rotation oscillation, using a Modular Compact Rheometer (MCR92, Anton Paar), at 37ºC with a 25 mm diameter parallel measuring plate (PP25). Hydrated hydrogel samples were cut into 25 mm diameter disks, with a height between 2 and 3 mm. 5 mL of DD water was added to the dish where the hydrogel was placed. Before testing, the specimens were held at the measurement gap for 15 min to eliminate thermal and shear artefacts.

An amplitude sweep test was carried out at a fixed frequency (1 Hz), to determine the range of strains at which the material maintains its elastic nature (linear viscoelastic regime, LVE). All subsequent tests were performed at a fixed shear strain within the LVE (0.1%). The hydrogels

were also submitted to a frequency sweep (FS) measurement, between 0.1 to 100 Hz. Finally, isothermal time test (ITT), was performed for 1 hour, with constant frequency (1 Hz).

The steady shear rate viscosity of the SSF was also measured, for a shear rate range of 0-100 s^1, at both room temperature and normal human body temperature (37ºC). This measurement was performed using a cone-plate geometry (CP50).

2.9. Hardness

A Shore A Durometer was used to measure the hardness value of the hydrogel materials. Cylindrical samples (h=4mm; ϕ=8mm) for each condition were tested for the Shore A hardness value.

2.10. Wettability

The water contact angle (CA) of the hydrogel was measured at room temperature using the captive bubble method. Hydrated samples were fixed to a support and placed upside-down inside a quartz glass liquid cell, filled with DD water, and an air bubble was created at the hydrogel surface. Pictures of the bubbles were taken with a video camera (JAI CV-A50) connected to an optical microscope (WildM3Z) and to a frame grabber Data Translation DT3155. Images were acquired at pre-defined times during 30 s. The value of the CA was obtained by image analysis of the last picture of each bubble, using the ADSA-P software (Axisymmetric Drop Shape Analysis Profile, Toronto University) which fits a theoretical profile based on the Laplace capillarity equation to the experimental bubble profile. Images of 10 bubbles were captured in 3 different samples of for each material condition, for a total of 30 bubbles (n=30).

2.11. Tribology

Hydrated hydrogel samples were tested in a pin-on-disk tribometer (TRB3, Anton Paar), in reciprocal oscillating mode at room temperature, for 2500 cycles, full amplitude of 4.0 mm and a sliding velocity of 8.0 mm/s. The data was collected as a function of time using the InstrumX 9.0.12 software, with acquisition frequency of 10 Hz. The total duration of the assays was 1 hour and 5 minutes. As the counter body, 6 mm cylindrical porcine cartilage pins were used. The NS material was tested at a load of 10, 20 and 30 N, corresponding to a Hertzian contact pressure of 0.354, 0.707 and 1.061 MPa, respectively. The samples were completely immersed in DD water and in SSF, using a liquid cell. The SZ materials were tested only at a 30 N load and immersed in SSF, to simulate natural lubrication at high loads (boundary lubrication regime) [21]. Samples and cartilage pins were immersed for 1 hour in SSF prior to testing. At least three replicates were performed for each condition.

2.12. Surface Morphology

Characterization of the PVA-Zylon hydrogel's morphology, after the tribological testing (30 N load), was done in a Hitachi S-2400 scanning electron microscope (SEM). The hydrogels were carefully cut around the areas where wear marking was evident. Afterwards the samples were dried at 45 ºC for 48 hours, and coated with Au/Pd (100 nm) for conductivity purposes using a sputter coater and evaporator (Polaron Quorum Technologies, Laughton, East Sussex, UK). Each sample was observed inside and outside the wear marks, at magnifications ranging from 150x to 5000x.

2.13. Irritability

Fertilized hen's eggs were incubated at 37 $\pm$ 0.5ºC, with 60 ± 2% relative humidity (Intelligent Incubator 56S) for 8 days. On the 9th day, a small opening was cut on the egg shell surface, using a rotary saw and a scalpel. The inner membrane was moistened with a 0.9% NaCl solution, and the eggs were further incubated for 30 minutes. The inner membrane was then carefully removed, ensuring no damage occurred to the underlying blood vessels, thus exposing the chorioallantoic membrane (CAM). Triplicate samples for each sterilization type as well as non sterilized hydrogels were placed directly on the CAM, and left for 5 minutes while visually inspecting for signs of lysis, hemorrhage or coagulation, to calculate the IS. 300 µl of NaOH (0.1 M) and 0.9% NaCl solutions were used as positive and negative controls, respectively.

2.14. Citotoxicity

Cytotoxicity assays were conducted, using the extract test method, in accordance with ISO 10993-5. Human chondrocyte cells, cultured in DMEM were counted with a hemacytometer to ensure at least 0.5x10^5 cells could be placed in each well. 400 µL of cell suspension were added to a 24 well plate, in quadruplicate for each sterilization type. A positive (DMEM + 10% DMSO) and negative (DMEM only) control were also tested. Hydrogel samples from each sterilization type were placed in a flask with DMEM media in a 3 cm^2/mL concentration, to obtain extracts containing leachouts of the hydrogels. The extracts and cells were left for 24 hours at 37ºC in a humified 5% CO_2 incubator, after which time the DMEM media was removed and replaced with the same amount of sample extract. After 48 hours the cultures were again evaluated and photographed to qualitatively assess cell viability, morphology and eventual cell detachment.

MTT(3-(4,5-Dimethylthiazol-2-Yl)-2,5-Diphenyltetrazolium Bromide) assay was performed to quantify cell viability. The liquid media was substituted with 300 µL of 10% MTT solvent solution on simple DMEM medium (serum-free). Three empty wells were filled with the same amount of solution for an absorbance control. The cells were left for 3 hours to react, and then 450 µL of pure MTT solvent (4 mM HCL, 0.1% IGEPAL in isopropanol) was added to each well. The plates were wrapped in foil, agitated in a orbital-shaker for 15 minutes and up-down pipetting was performed to fully dissolve the MTT formazan crystals. Finally the absorbance of the samples was read at 595 nm, using a microplate reader (Microplate reader AMP Platos R 496 AMEDA, AMP diagnostics), and the relative quantification of cell viability was normalized to the negative control.

2.15. Cell Adhesion

Two small samples from each sterilization method were placed in a 12 well plate after carefully drying their surface with a sterilized paper towel. 20 µL of concentrated

cell suspension was carefully placed at the top of each sample, and left for 1 hour at the incubator (at 37ºC, 5% CO2) to ensure proper cell adhesion. Afterwards, the samples were immersed in approximately 1.5 ml of DMEM medium and further incubated. After 22 days the samples were visually inspected in the microscope for signs of cellular adhesion.

3. Results

3.1. Sterility Tests

Photographs of the cultured SZ samples and controls are present in Figure 1. Observation of the incubated flasks demonstrated that all SZ methods effectively ensured sterility. After 14 days of incubation, no microorganisms grew in the mediums, contrary to what occurred in the positive controls. No difference was observed between the MW SZ with 3 and 5 minutes of exposure, so all further testing on MW samples was performed with an exposure time of 3 minutes.

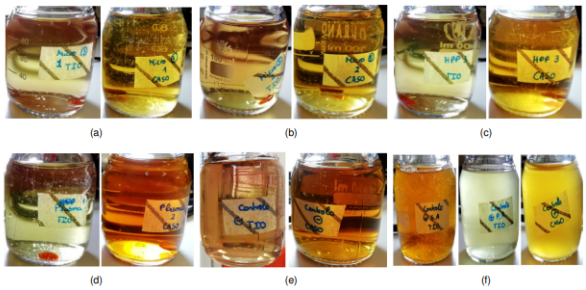

Figure 1: CASO and TIO culture medium after 14 days of incubation of the PVA-Zylon hydrogel samples after (a) MW 3 min b) MW 5 min , (c) HHP, (d) plasma SZ methods; (e) Negative controls, (f) Positive controls.

3.2. Microstructural Analysis

Figure 2 shows the comparison between the FTIR spectrums of non-sterile (NS) and SZ samples. The SZ procedures were found to induce changes in peak intensity, indicating a variation in the number of certain molecular bonds.

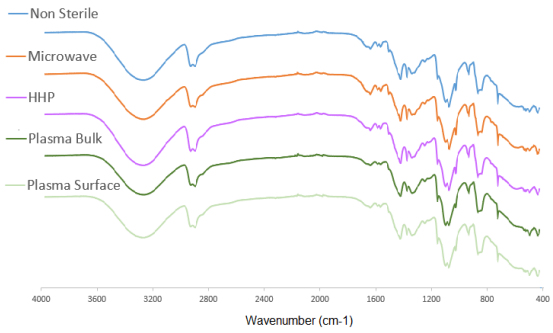

Figure 2: FTIR-ATR spectra of the non-sterilized and sterilized PVA-Zylon hydrogels

The samples submitted to MW show higher intensities in peaks attributed to C=O and C=N (1500-1700 cm^{-1}) as well as C=C (1495 cm^{-1}) groups compared to NS samples. A very slight increase in C–C and C–O–C peak intensity (i.e. 1141 cm^{-1}) can also be seen. Meanwhile areas associated with -OH (3200-3400 cm^{-1}) and C-O (1088 cm^{-1}) groups display a lower intensity. Regarding C–H and CH_2 bonds, in the peaks associated with these groups (2850-2950, 1430, 1132 and 705 cm^{-1}) the MW and NS samples' spectra overlapped.

HHP samples showed increased intensity in peaks associated with -OH (3200-3400 cm^{-1}), C-H (2850-2950 cm^{-1}), C-N-C (1500-1100 cm^{-1}), CH_2 (1430, 1132 and 916 cm^{-1}), C-O-C (1141 and 1016 cm^{-1}), C-O (1088 cm^{-1}) and C-C (850 cm^{-1}) groups. A small increase can also be seen at 1495 cm^{-1}, attributed to C=C stretching. In all other regions, the HHP spectrum overlapped the NS'.

Plasma SZ samples show reduced peak intensity across the whole FTIR spectrum, with the bulk sample showing overall lower intensity than the surface. The only peaks where plasma samples show slightly higher intensities than NS are those associated to C-O stretch (1088 cm^{-1}). Surface samples also showed higher intensity at peaks attributed to C-C and C-O-C stretching (1141 cm^{-1}).

3.3. Swelling

The results of the swelling behaviour of the hydrogels are presented in Figure 3. A sharp rise in SC can be observed in the first 5 hours and, after 25 hours of hydration, the hydrogels seem to reach equilibrium. HHP and plasma SZ seem to have no significant effect on this property. Meanwhile the MW samples presented a high heterogeneity evidenced by the error bars. The dispersion of the results doesn´t allow for an appropriate conclusion on the effects of MW irradiation on the SC of the hydrogels.

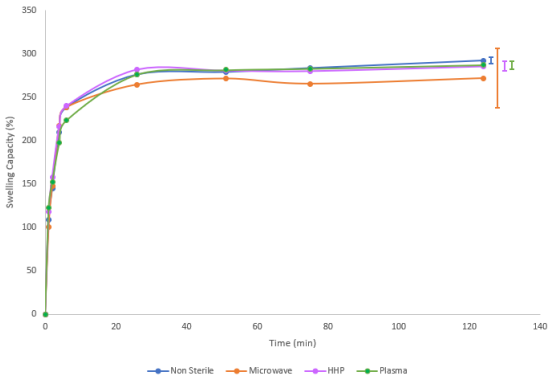

Figure 3: SC of the non-sterilized and sterilized PVA-Zylon hydrogels. The error bars represent the ± mean standard deviations (n=3).

Similar results were obtained in the WC of the hydrogels, even after increasing the sample number (n=7). All hydrogels showed WC values between 73.1 $\pm$ 4.0 (MW) and 74.5 $\pm$ 0.3 (NS).

3.4. Compression

A typical stress-strain curve for each of the SZ and NS hydrogels is shown in Figure 4. The NS hydrogels were found to have an average E_c (1% strain) of 0.25 ± 0.08. HHP and plasma SZ had no effect on this property, displaying E_c of 0.25 ± 0.06 and 0.26 ± 0.05 respectively. The MW irradiated samples on the other hand, show more

than a double increase of E_c (0.55 ± 0.10).

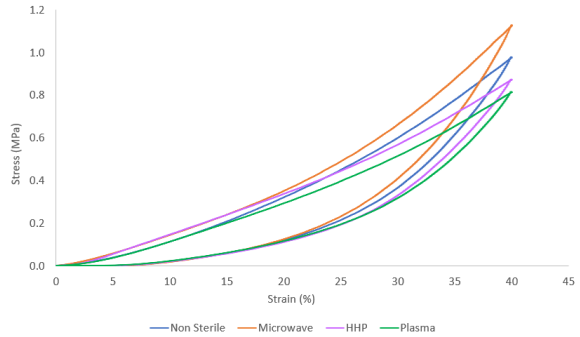

Figure 4: Typical compressive stress-strain curves of non-sterilized and sterilized PVA-Zylon hydrogels.

Figure 5 depicts the compressive E_ϵ between 5-35% strain. MW irradiation increased the compressive stiffness of the hydrogels, across the whole tested strain range, from a minimum increase of 5.29%, up to a maximum of 32.41%. The other two procedures show a slightly different behaviour to those of the NS and MS samples, with a less linear increase. At lower strains, up to ≈15%, the HHP samples present the highest E_ϵ, with increases of up to 58% compared to the NS samples. However, at higher strains, HHP actually shows E_ϵ up to 13.57% lower than the NS samples. A similar behaviour was observed in plasma treated samples. While at lower strains, the plasma samples do show a slightly higher E_ϵ than the NS, this increase is significantly lower when compared to the other methods (maximum 7.86%). As the strain increases, the plasma samples show the lowest compressive stiffness of all the tested materials, lowering the E_ϵ by up to 17.67% compared to the NS samples.

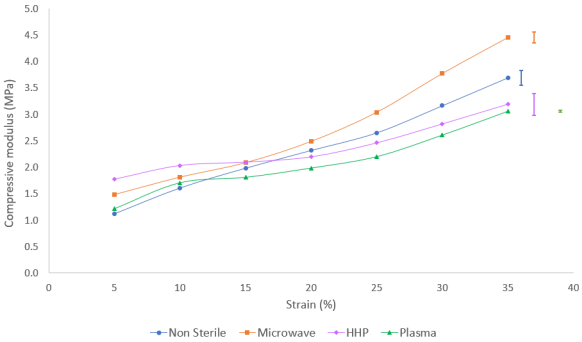

Figure 5: Comparison of compressive tangent modulus of sterilized and unsterilized samples obtained at different strains (5–35%). Error bars represent the ± standard deviations (n=2).

3.5. Tension

Typical tensile stress-strain curves for each condition are displayed in Figure 6. All SZ methods appear to have a significant effect on the tensile resistance of the hydrogels. MW, HHP and plasma sterilization increased the E_t (1% strain) to 177%, 138% and 152% of the original value, respectively. While all methods also increased the average stress at break, the maximum strain actually diminished in MW and HHP sterilized samples.

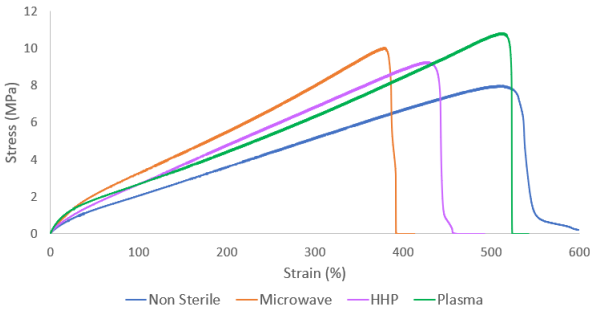

Figure 6: Typical tensile stress-strain curve of non-sterilized and sterilized PVA-Zylon hydrogels.

The variation of the tensile E_ϵ from 1-35% strain is shown in Figure 7. All SZ methods had positive effects on the tensile resistance of the PVA-Zylon hydrogels, with an increase in tensile E_ϵ across the tested strains. MW irradiation especially, shows very significant increases, ranging between 46% and 78%.

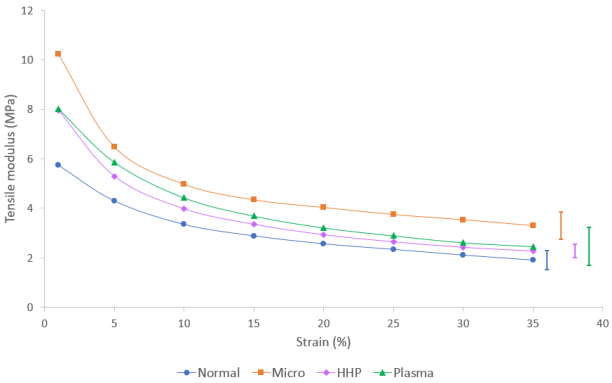

Figure 7: Comparison of tensile tangent modulus with increasing strain, on sterilized and unsterilized samples. The error bars represent the ± mean standard deviations (n=4).

3.6. Rheology

The LVE of the PVA-Zylon hydrogels was determined and a shear strain of 0.1% was the proposed optimal working strain for this material and was used for all subsequent testing.

Figure 8 shows the angular FS curves obtained within the LVE. For all hydrogels G' is almost 1 order of magnitude larger than G" across the tested frequency range, indicative that the PVA-Zylon hydrogels show a rigid network, with elastic rather than viscous response to stress. Overall, the effect of the angular frequency on G' and G" does not seem to be very significant. Comparing the hydrogels, the non-sterilized samples showed the lowest G' and G", while MW subjected hydrogels demonstrated the highest values.

In all samples, the ITT measurements found no significant changes in either G' or G" during the tested time range (1 hour) indicating the material does not lose its elasticity over prolonged stress (Figure 9). All hydrogels presented a calculated δ close to 0º, further indicative of predominantly elastic contributions. The plasma treated samples show δ almost equal to the NS hydrogel (3.82º

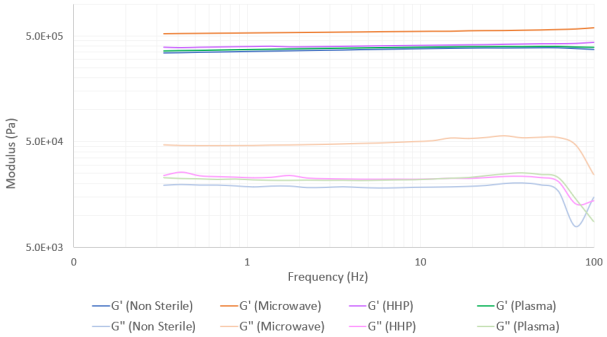

Figure 8: Frequency sweep curve (0.1–100 Hz) of the PVA-Zylon hydrogels, within the LVE (0.1% strain).

and 3.79º, respectively), while HHP samples showed the lowest δ (2.47º), indicating a lower amount of dissipated energy. MW irradiation slightly increased the δ (6.51º), suggesting a higher viscous dissipation of energy.

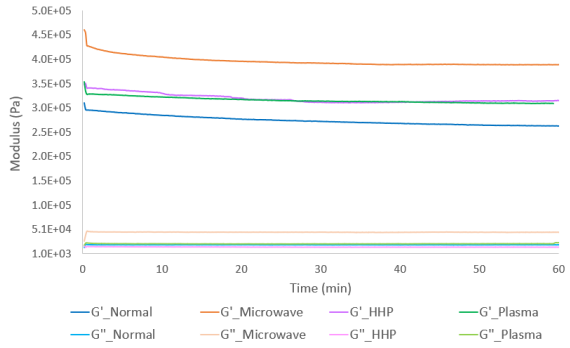

Figure 9: Storage (G') and loss modulus (G") as function of time (1 hour), at 0.1% strain and frequency of 1 Hz, for non-sterilized and sterilized PVA-Zylon hydrogels.

3.7. Hardness

Regarding Shore A hardness, all the SZ procedures had different effects on the hydrogel. The NS samples presented a hardness of 45. MW irradiation and HHP increased this value to 54 and 47, respectively. Meanwhile, the plasma treated samples lowered the hardness to 42.

3.8. Wettability

No significant changes were observed in the wettability of the hydrogel after undergoing MW, HHP or plasma SZ. The largest variation was 3.13%, between the NS hydrogel and one that underwent MW irradiation. All hydrogels show a hydrophilic behaviour, with a CA between 38.9º and 40.1º.

3.9. Tribology

DD water and SSF were tested as lubricants. The viscosity of the SSF solution showed a value of 17.52 ± 0.65 mPa.s at room temperature (22.7ºC) and slightly decreased to 14.07±1.18 at 37ºC. Higher loads led to a clear increase in the measured CoF in both types of lubricant. The CoF was lower for all tested normal forces with SSF as lubricant. SSF resulted in a CoF 53.3% lower at 10 N, 37.7% lower at 20 N, and 3.5% lower at 30 N than that obtained with DD water.

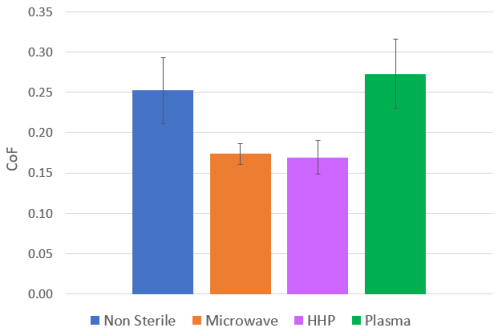

Figure 10: Maximum CoF of non sterilized and sterilized PVA-Zylon hydrogels against porcine cartilage, obtained by reciprocating analysis after 2500 cycles of linear friction, using SSF as lubricant. The error bars represent the ± standard deviations (n= 3).

The maximum CoFs of the sterilized and non-sterilized hydrogels are shown in Figure 10. MW and HHP SZ reduced the maximum CoF of the hydrogels by 31.26% and 32.94% respectively, while plasma SZ increased the CoF by 8.11%, when compared to the NS hydrogel.

3.10. Surface Morphology

Surface analysis of the SZ and NS hydrogels was performed by SEM (Figure 11). The MW and HHP samples appear to show a slightly more homogenous and smooth surface. On the other hand, plasma SZ seems to have increased roughness of the samples. Moreover, some samples showed the presence of etching-derived holes (Figure 12). A large distribution of holes can be seen across the hydrogel's morphology, with different stages of etching.

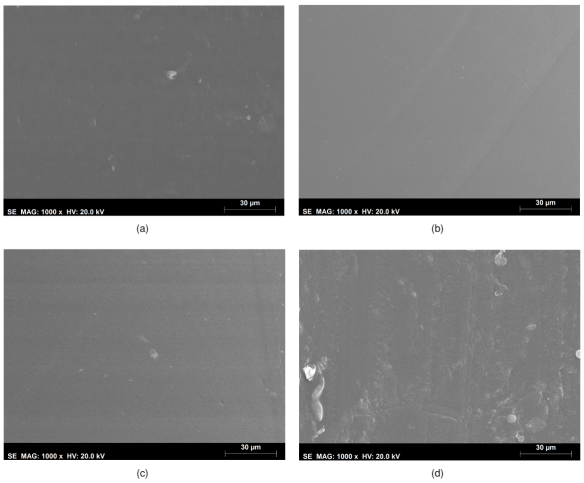

Figure 11: SEM micrographs of the PVA-Zylon hydrogels. (a) Non sterile; (b) Microwave; (c) HHP; (d) Plasma. All images were acquired with 1000x magnification.

SEM images were taken inside the wear tracks caused by tribological testing (Figure 13). The NS samples show a more delaminated surface, while the SZ samples show a wavy like pattern throughout the track, more striking for the plasma treated hydrogel.

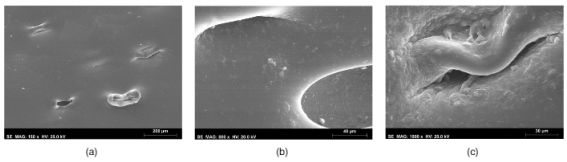

Figure 12: SEM micrographs of plasma sterilized PVA-Zylon hydrogels, at different magnifications, (a) 150x; (b) 800x; (c) 1000x

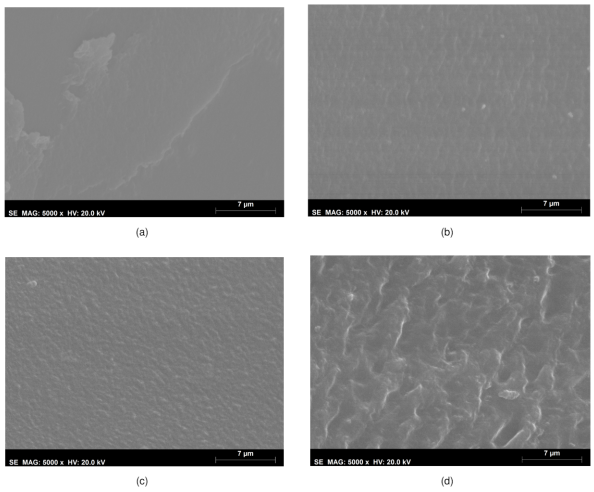

Figure 13: SEM micrographs of the PVA-Zylon hydrogels inside the tracks after the tribological tests. (a) Non sterile; (b) Microwave; (c) HHP; (d) Plasma. All images were acquired with 5000x magnification.

3.11. Irritability

Macroscopic photographs of the CAM after 5 minute of direct contact with the NS and SZ PVA-Zylon hydrogels are presented in Figure 14. In the positive control, the addition of NaOH caused severe irritation, with an almost instant hemorrhage and coagulation (Figure 14,b). Contrarily, the effects of the hydrogel samples were similar to the negative control, with no visual signs of lysis, hemorrhage or coagulation, as such, the IS was equal to 0.

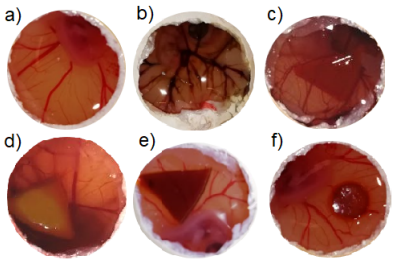

Figure 14: Chorioallantoic membrane images after 5 minute of exposure to the hydrogel samples. a) negative control (NaCl 0.9%); b) positive control (NaOH, 1 M); c) non-sterilized hydrogel; d) microwave; e) HHP; and f) plasma subjected hydrogels.

3.12. Citotoxicity and Cell adhesion

Visual inspection of the cultured chondrocytes shows a greater number of cells on the wells containing extracts from plasma treatment, than from the other methods. The MMT assay confirmed these results (Figure 15), with extracts from the hydrogels after MW and HHP sterilization showing lower percentage of viable cells (68.75% and 77.6%, respectively) when compared to the negative controls. Plasma, on the other hand, showed excellent results, with a cell viability of 98.57%. Chondrocytes were seen be thriving and adhered to samples sterilized by the three methods after 22 days.

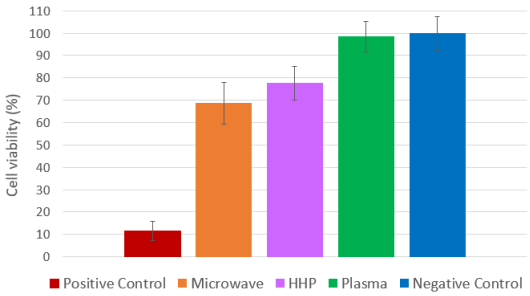

Figure 15: Chondrocyte cell viability (%) determined by the MTT assay, after 48 hours of exposure to the hydrogel sample extracts. The relative cell viability is presented as percentage of negative control cells. The error bars represent the ± standard deviations (n=4*2).

4. Discussion

Table 1 shows the measured properties of the NS PVA-Zylon hydrogels compared to those of natural AC. The hydrogel displayed adequate compressive, tensile and shear resistances, while maintaining a WC well within the range measured for articular cartilage. The reinforcement of the PVA matrix with Zylon nanofibers allowed for a superior compressive resistance compared to monopolymer, cast-dried PVA hydrogels [23]. Unfortunately, some properties still fell short of the natural tissue, particularly the Shore A hardness and CoF. The results also showed that each of the SZ procedures induced changes in the hydrogel.

FTIR analysis evidenced that the main effect of the MW process is the increase in the amount of double bonds (C=O, C=N, C=C) in the hydrogel network. Intermolecular bonding is also slightly improved, evidenced by the small increase in C–C and C–O–C peak intensity. These results are congruent with other studies on the effect of MW irradiation on PVA and PVA/graphene nanocomposites [24]. Similar results to those obtained in this thesis have also been found in PVA samples after gamma irradiation [25, 26]. The MW procedure is thought to rupture the side chains of the PVA polymer, evidenced by the lower intensity in areas associated with -OH and C-O and the lack of effects in C–H and CH_2 bonds. This could facilitate the segmental motion and chains become more free to realign [24], which ultimately can led to additional cross-linking.

In the case of HHP, the procedure increased the amount of hydrogen and single bonds across the PVA-Zylon hydrogel matrix. Meanwhile, double bonding doesn´t seem to be very prevalent. Studies on HHP processing on pre-crosslinked hydrogels are in agreement with these results, with HHP treatment increasing the -OH stretching peaks in PVA composites [27]. The extreme pressures during the HHP process may cause breakage of old H-bonds and the creation of new intra/inter-molecular bridges between the polymer molecules.

Table 1: Biomechanical properties of non-sterilized PVA-Zylon hydrogel and natural articular cartilage

Property	PVA-Zylon	Articular Cartilage	Source
E_c (MPa)	0.25	0.24–0.85	[22]
E_t (MPa)	5.74	5–25	[22]
G* (MPa)	0.3	0.2–2.5	[22]
Tensile strength (MPa)	7.8	0.8-25	[22]
Shore A Hardness	45	87.5	[6]
WC (%)	75	65-80	[2]
CoF	0.25	0.001-0.03	[3]

Meanwhile, plasma treated samples evidence a general rupture of bonds in the hydrogel structure. New oxygen containing groups (C-O) also appear in the plasma treated hydrogels, which is in agreement with other studies [28]. During plasma treatment, the inert argon plasma is thought to break the chemical bonds of the hydrogel's surface and create radicals. When the material is exposed to air, these radicals can then form polar bonds with oxygen atoms in the atmosphere [29]. Some of these C–O groups could then form bonds between other free carbon atoms, inducing C–O–C intermolecular bonding. This is more clear for the surface plasma sample than for the bulk sample, as expected, being plasma sterilization process a more superficial method.

Regarding the mechanical properties, MW irradiation significantly increased all the measured properties. These results are congruent with the increase in double bonding evidence by the FTIR spectrum. The higher increases of compressive E_c at lower compressive strains (1%), where fluid flow plays a big role [30], coupled with the higher values for δ which indicate a higher viscous dissipation of energy could also entail an improved interaction between polymer and interstitial water.

HHP treatment also increased the shear and tensile moduli, as well as in the Shore A hardness of the samples, as expected due to the higher amount of single bonds in the hydrogels' matrix. At low compressive strains (5–15%) the HHP hydrogels actually showed the best compressive stiffness. However, at higher compressive strains, the modulus decrease below NS samples. Weaker bonds could be the cause for this behavior, hindering the hydrogels' capacity to resist stronger stresses.

Plasma sterilized hydrogels showed contradicting results in the mechanical testing. The bond degradation evidenced in the FTIR spectrum could explain the observed reduction in compressive stiffness at high loads and lower hardness. However, the results from the tensile testing indicate that plasma treatment actually improved the hydrogel's tensile resistance across the whole tested strain, while maintaining a maximum strain close to the NS samples. The shear resistance was also improved after plasma treatment but the δ remained unaltered. One possible cause for these results is that the plasma treatment mainly affects the PVA chains rather than the Zylon fibers, which are thought to play a bigger role in tensile resistance, owing to the extremely high tensile modulus of the fibers (180 GPa). In fact, low power Ar plasma treatment of Zylon fibers was found to increase their interfacial adhesions with resin matrices while preserving their tensile properties [29]. An increased interfacial adhesion is in agreement with the observed increase in C-O-C bonds.

Concerning the tribological behaviour, as expected, the SSF less viscous than SF [4], due to the lack of some of the SF lubricant molecules. Still, the SSF had a higher viscosity than water (0.9321 mPa.s at 23ºC, according to IAPWS 2008). Consequently, SSF used as lubricant resulted in lower CoF values than when using DD water. The results also indicate that the lubrication mechanism of fluid is more significant at lower loads, correlated with the prevalence of the BL regime at higher loads.

Both MW and HHP SZ led to similar results in both the CoF and SEM micrographs. The wavy-like pattern of the wear tracks is similar to the one observed in other tribological studies of PVA hydrogels against bovine cartilage [31]. The reduction in the CoF could be correlated with the increase in bonding evidenced in the FTIR analysis. Accordingly, the smoothing effect has also been observed previously after MW irradiation [24]. Regarding HHP, the effects of extreme pressure could also explain the decrease in CoF, smoothing out micro-asperities in the hydrogel surface, thus reducing roughness.

On the other hand, plasma led to an increase of the CoF, and SEM analysis depicted a rougher surface, which are in line with the bond degradation and decrease in hardness. Furthermore, it was possible to observe the presence of etching-derived holes, common side effect of the plasma procedure [19]. Other researchers also found an increase in roughness after Ar plasma treatment of PVA-chitosan films [28].

Finally, in biocompatibility tests, all of the tested samples were non-irritant (IS=0). The citotoxicity results, however, varied between the SZ methods. ISO 10993-5:2009 states that for a material to be considered non-citotoxic, it must allow for a cellular viability $\geq$70%. While HHP and plasma SZ hydrogels fall within the necessary range, MW SZ samples are right at the threshold of this parameter. However, the variability of the results was significant. Moreover, it was possible to observe that the chondrocytes cultured in microwave sample extracts possessed the correct morphology after 48 hours of culture and the cells were seen to adhere and thrive, after 22 days of culture on top of hydrogel samples that underwent MW SZ. This leads to think that MW irradiation, while not showing the best results, can still be considered non-citotoxic.

5. Conclusions

The SZ methods tested in this work showed to be effective and present advantages over conventional SZ procedures, such as autoclaving and gamma-ray irradiation which require lengthy processing times and specialized equipment and staff.

MW irradiation proved to be the most adequate to sterilize the PVA-Zylon hydrogels. It has an highly penetra-

tive effect and can achieve high temperatures with great efficiency and speed. MW allowed for a terminal SZ at reduced exposure times, while it improved the properties of the hydrogel.

The HHP procedure also showed some promising results, producing a slightly stiffer material, with superior tribological behaviour. Both its tensile and shear resistance improved over the NS hydrogels, but not as much as the MW procedure. While the mechanical resistance of the hydrogels at higher loads decreased after HHP treatment, it was still within the required range for AC. Moreover, HHP samples showed the best compressive stiffness at lower loads. However, HHP requires specialized and expensive equipment, and is not readily available, hindering its worldwide application.

Lastly, plasma sterilization showed the best biocompatibility, but its effects on the properties of the hydrogel were less than adequate. Etching of the surface occured, thus affecting the CoF and wear. While the shear and tensile moduli actually increased, the compressive stiffness and hardness of the hydrogel significantly decreased.

Overall, the produced PVA-Zylon hydrogels have shown to be promising materials for cartilage substitution, with mechanical properties within the range measured for AC. However, the tribological behavior still falls slightly short, and further effort should be made to optimize it. SZ, being already required, can also be tailored to favorably improve the hydrogels properties

References

[1] Chiara Gentili and Ranieri Cancedda. Cartilage and bone extracellular matrix. *Current pharmaceutical design*, 15:1334–48, 02 2009.

[2] A.R. Armiento, M.J. Stoddart, M. Alini, and D. Eglin. Biomaterials for articular cartilage tissue engineering: Learning from biology. *Acta Biomaterialia*, 65:1–20, 2018.

[3] Sabrina Jahn, Jasmine Seror, and Jacob Klein. Lubrication of articular cartilage. *Annual Review of Biomedical Engineering*, 18(1):235–258, 2016. PMID: 27420572.

[4] S. More, A. Kotiya, A. Kotia, S.K. Ghosh, L.A. Spyrou, and I.E. Sarris. Rheological properties of synovial fluid due to viscosupplements: A review for osteoarthritis remedy. *Computer Methods and Programs in Biomedicine*, 196:105644, 2020.

[5] Alice J. Sophia Fox, Asheesh Bedi, and Scott A. Rodeo. The basic science of articular cartilage: Structure, composition, and function. *Sports Health*, 1(6):461–468, 2009.

[6] Gunter Spahn, Holger Plettenberg, Horst Nagel, Enrico Kahl, Hans Michael Klinger, Thomas Mückley, Manfred Günther, Gunther O. Hofmann, and Jürgen A. Mollenhauer. Evaluation of cartilage defects with near-infrared spectroscopy (nir): An ex vivo study. *Medical Engineering Physics*, 30(3):285–292, 2008.

[7] Philippe Abdel-Sayed and Dominique Pioletti. Strategies for improving the repair of focal cartilage defects. *Nanomedicine (London, England)*, 10:2893–905, 09 2015.

[8] Douglas Jackson, Mark Scheer, and Timothy Simon. Cartilage substitutes: Overview of basic science and treatment options. *The Journal of the American Academy of Orthopaedic Surgeons*, 9:37–52, 01 2001.

[9] Maribel Baker, Steven Walsh, Zvi Schwartz, and Barbara Boyan. A review of polyvinyl alcohol and its uses in cartilage and orthopedic applications. *Journal of biomedical materials research. Part B, Applied biomaterials*, 100:1451–7, 07 2012.

[10] Won ill Cha, Suong hyu Hyon, Masanori Oka, and Yoshito Ikada. Mechanical and wear properties of poly(vinyl alcohol) hydrogels. *Macromolecular Symposia*, 109:115–126, 1996.

[11] Meiling Chen, Yuncheng Mo, Zesheng Li, Xiankun Lin, and Qiang He. Poly(p-phenylenebenzobisoxazole) nanofiber layered composite films with high thermomechanical performance. *European Polymer Journal*, 84:622–630, 2016.

[12] Parth Chansoria, Lokesh Narayanan, Madison Wood, Claudia Alvarado, Annie Lin, and Rohan Shirwaiker. Effects of autoclaving, etoh, and uv sterilization on the chemical, mechanical, printability, and biocompatibility characteristics of alginate. *ACS Biomaterials Science Engineering*, XXXX, 07 2020.

[13] B.J. Parsons. *Sterilisation of healthcare products by ionising radiation: Principles and standards*, pages 56–70. 12 2012.

[14] Michael D. Rohrer, Mark A. Terry, Ronald A. Bulard, Donald C. Graves, and Elaine M. Taylor. Microwave sterilization of hydrophilic contact lenses. *American Journal of Ophthalmology*, 101(1):49–57, 1986.

[15] Hosahalli S. Ramaswamy Jasim Ahmed. Microwave pasteurization and sterilization of foods. In *Handbook of Food Preservation*, chapter 28. CRC Press, 3rd edition edition, 2014.

[16] Maryam Yaldagard, Seyed Mortazavi, and Farideh Tabatabaie. The principles of ultra high pressure technology and its application in food processing/preservation: A review of microbiological and quality aspects. *African Journal of Biotechnology*, 7:2739–2767, 09 2008.

[17] Ana Topete, Carlos Pinto, Maria Barroso, Jorge Saraiva, Isabel Barahona, Benilde Saramago, and Ana Serro. High hydrostatic pressure (hhp) as sterilization method for drug-loaded intraocular lenses. *ACS Biomaterials Science Engineering*, XXXX, 06 2020.

[18] Liqing Yang, Jierong Chen, and Junling Gao. Low temperature argon plasma sterilization effect on pseudomonas aeruginosa and its mechanisms. *Journal of Electrostatics*, 67:646–651, 07 2009.

[19] Low-temperature sterilization using gas plasmas: a review of the experiments and an analysis of the inactivation mechanisms. *International Journal of Pharmaceutics*, 226(1):1–21, 2001.

[20] Yan Shi, Jianliang Li, Dang Xiong, Long Li, and Qibin Liu. Mechanical and tribological behaviors of pva / paam double network hydrogels under varied strains as cartilage replacement. *Journal of Applied Polymer Science*, 138:50226, 11 2020.

[21] Michelle Blum and Timothy Ovaert. A novel polyvinyl alcohol hydrogel functionalized with organic boundary lubricant for use as low-friction cartilage substitute: Synthesis, physical/chemical, mechanical, and friction characterization. *Journal of biomedical materials research. Part B, Applied biomaterials*, 100B:1755–63, 10 2012.

[22] Christopher Little, Nahshon Bawolin, and Xiongbiao Chen. Mechanical properties of natural cartilage and tissue-engineered constructs. *Tissue engineering. Part B, Reviews*, 17:213–27, 03 2011.

[23] Andreia Oliveira, Oumar Seidi, Nuno Ribeiro, Rogério Colaço, and Ana Serro. Tribomechanical comparison between pva hydrogels obtained using different processing conditions and human cartilage. *Materials*, 12:3413, 10 2019.

[24] Hafiz Afzal, Farrukh Shehzad, Mukarram Zubair, Omer Bakather, and Mamdouh Al-Harthi. Influence of microwave irradiation on thermal properties of pva and pva/graphene nanocomposites. *Journal of Thermal Analysis and Calorimetry*, 139, 06 2019.

[25] N. El-Sawy, Magda El-Arnaouty, and Ashraf Abdel Ghaffar. γ-irradiation effect on the non-cross-linked and cross-linked polyvinyl alcohol films. *Polymer-plastics Technology and Engineering - POLYM-PLAST TECHNOL ENG*, 49:169–177, 01 2010.

[26] Narendra Bhat, Mandar Nate, M. Kurup, V. Bambole, and Sunil Sabharwal. Effect of γ-radiation on the structure and morphology of polyvinyl alcohol films. *Nuclear Instruments Methods in Physics Research Section B-beam Interactions With Materials and Atoms - NUCL INSTRUM METH PHYS RES B*, 237:585–592, 08 2005.

[27] Zixuan Lian, Yifeng Zhang, and Yanyun Zhao. Nano-tio2 particles and high hydrostatic pressure treatment for improving functionality of polyvinyl alcohol and chitosan composite films and nano-tio2 migration from film matrix in food simulants. *Innovative Food Science Emerging Technologies*, 33, 11 2015.

[28] Ramhari Paneru, se hoon Ki, Pradeep Lamichhane, Linh Nguyen, Bishwa Adhikari, Il Jeong, Sohail Mumtaz, Jinsung Choi, Jae-Sung Kwon, and Eun Choi. Enhancement of antibacterial and wettability performances of polyvinyl alcohol/chitosan film using non-thermal atmospheric pressure plasma. *Applied Surface Science*, 532:147339, 08 2020.

[29] Dong Liu, Ping Chen, Mingxin Chen, and Zhe Liu. Surface modification of high performance pbo fibers using radio frequency argon plasma. *Surface and Coatings Technology*, 206:3534–3541, 04 2012.

[30] Jörg Eschweiler, Nils Horn, Bjoern Rath, Marcel Betsch, Alice Baroncini, Markus Tingart, and Filippo Migliorini. The biomechanics of cartilage—an overview. *Life*, 11:302, 04 2021.

[31] V.M. Sardinha, L.L. Lima, W.D. Belangero, C.A Zavaglia, V.P. Bavaresco, and J.R. Gomes. Tribological characterization of polyvinyl alcohol hydrogel as substitute of articular cartilage. *Wear*, 301(1):218–225, 2013. Wear of Materials 2013.